Insight into miscibility behaviour of cellulose ester blends with *N*-vinyl pyrrolidone copolymers in terms of viscometric interaction parameters

Kazuki Sugimura, Yoshikuni Teramoto, and Yoshiyuki Nishio*

Division of Forest and Biomaterials Science, Graduate School of Agriculture, Kyoto University, Kyoto 606-8502, Japan

*To whom correspondence should be addressed.

E-mail: ynishio@kais.kyoto-u.ac.jp. Tel.: +81 75 753 6250. Fax: +81 75 753 6300.

Abstract: We previously offered miscibility maps for blend systems of cellulose esters (CEs) including cellulose acetate (CA), propionate (CP), and butyrate (CB) with vinyl copolymers containing an *N*-vinyl pyrrolidone (VP) unit, i.e., poly(*N*-vinyl pyrrolidone-*co*-vinyl acetate) (P(VP-*co*-VAc)) and poly(*N*-vinyl pyrrolidone-*co*-methyl methacrylate) (P(VP-*co*-MMA)); the maps were constructed based on data of thermal analysis as a function of the degree of ester substitution (DS) of the CE component and the VP fraction in the copolymer component. The blend system using CP among the three CEs imparted the largest region of miscible pairings with the vinyl copolymers, and both of the maps for the CP/P(VP-*co*-VAc) and CP/P(VP-*co*-MMA) systems comprised a "miscibility window" associated with the respective copolymer compositions at high DSs of >2.65. The present work was made to interpret the expansion of the miscible markings for the CP/copolymer systems in comparison with the cases using CA and CB, in terms of a Krigbaum-Wall interaction parameter (μ) obtained by solution viscometry for selective polymer pairs involved in the respective CE/copolymer blends. The results of μ measurements were in good accordance with the earlier miscibility estimations. The assessment of very small negative μ values (i.e., extremely weak repulsion) for CP/PVAc and CP/PMMA combinations and that of considerably larger negative μ values for PVP/PVAc and PVP/PMMA combinations enabled us to give a rational explanation for the CP systems. The strongly repellent character of the two different monomer units constituting the copolymers permits accession of the CP component (DS > 2.65) to them, which would be responsible for the advent of the miscibility window. Further expansion of the window observed when cellulose acetate propionate (CAP) was adopted instead of CP as the CE component was also well explained on the basis of a μ data indicative of additional intramolecular repulsion in the CAP side.

Keywords: Blend miscibility; Cellulose ester; Interaction parameter; Miscibility window; *N*-Vinyl pyrrolidone

Introduction

Organic esters of cellulose (CEs) are commercially important polymers over nearly a century. They are widely prevailing in application fields such as coating, drug delivery (excipients), molded plastics including biodegradable ones, fibers, optical films, and membranes and other separation media (Edgar et al. 2001; Rustemeyer 2004). For improvement in physical properties of CEs toward their further applications, the designing of high-functional multicomponent materials based on the cellulosics via graft copolymerization or polymer blending is a significant approach (Edgar et al. 2001; Nishio 2006; Yamaguchi 2010; Sugimura et al. in press). In the field of optical materials such as regulator or modulator of polarized light in modern displays, great attention of researchers has been focused on the delicate control of orientation birefringence and its wavelength dependence for CE-based films (Ohno and Nishio 2007a; Yamaguchi 2010; Yamaguchi et al. 2012; Yamanaka et al. 2013; Sugimura et al. 2013b; Hayakawa and Ueda 2015; Sugimura et al. in press). Especially, miscible polymer blending is practically useful to manipulate the physical properties and functions of CEs readily at the lowest cost possible. Therefore, there have been a number of fundamental and practical blend studies of CEs; the counter components to CEs are categorized into mainly two sorts of polymers, biodegradable aliphatic polyesters such as poly(3-hydroxybutyrate) and poly(ε-caprolactone) (Nishio et al. 1997; Edgar et al. 2001; Nishio 2006; Kusumi et al. 2008; Higeshiro et al. 2009), and synthetic vinyl polymers (Miyashita et al. 2002; Ohno et al. 2005; Nishio 2006; Ohno and Nishio 2006; Ohno and Nishio 2007a; Ohno and Nishio 2007b; Yamaguchi 2010; Yamaguchi et al. 2012; Yoshitake et al. 2013; Sugimura et al. 2013a; Sugimura et al. 2013b; Sugimura et al. in press).

Against the background stated above, the authors' group has recently performed basic characterization of miscibility and intermolecular interaction on binary blends of CEs with non-crystalline vinyl polymers, particularly poly(*N*-vinyl pyrrolidone) (PVP) and its random

copolymers (Miyashita et al. 2002; Ohno et al. 2005; Ohno and Nishio 2006; Ohno and Nishio 2007b; Sugimura et al. 2013a; Sugimura et al. 2013b). The CE component mainly used in the previous studies was cellulose acetate (CA), propionate (CP), or butyrate (CB) (Fig. 1a), and poly(*N*-vinyl pyrrolidone-*co*-vinyl acetate) (P(VP-*co*-VAc)) (Fig. 1b) or poly(*N*-vinyl pyrrolidone-*co*-methyl methacrylate) (P(VP-*co*-MMA)) (Fig. 1c) was the counter polymer component. Fig. 2a–c survey miscibility estimations for the blend systems of CA, CP, and CB, each combined with P(VP-*co*-VAc) (designated as CE/P(VP-*co*-VAc)) (Miyashita et al. 2002; Ohno and Nishio 2006; Sugimura et al. 2013a), by offering the miscibility map constructed as a function of the degree of ester substitution (DS) of CE and the copolymer composition of P(VP-*co*-VAc). The mappings were made based on thermal analysis (T_g detection) by differential scanning calorimetry (DSC). As can readily be seen by comparison of the three maps, the miscibility behaviour of CE/P(VP-*co*-VAc) blends is seriously affected by a small difference in alkyl chain-length (carbon number) of the acyl substituent in the employed CE. The CP system produced the largest miscible region.

<< **Figure 1 (a) & (b) & (c)** >>

<< **Figure 2 (a) & (b) & (c)** >>

Similar representations of miscibility estimations are given in Fig. 3 for two systems in which P(VP-*co*-MMA) was combined with either CA (Ohno and Nishio 2007b) or CP (Sugimura et al. 2013b); however, the mapping for CB/P(VP-*co*-MMA) blends is not made in this figure (see later discussion). Again interestingly, the miscible pairing region for the CP/P(VP-*co*-MMA) system is much larger than that for the CA/P(VP-*co*-MMA) system, with spreading to the upper right side of higher DS of CP and lower VP fraction of P(VP-*co*-MMA) in the map.

<< **Figure 3 (a) & (b)** >>

Using supplementary data from Fourier transform infrared (FT-IR) and solid-state NMR measurements, we have tentatively concluded that the CE/VP-containing copolymer

combinations assume miscible or immiscible behaviour according to the balance in effectiveness of the following four factors (Sugimura et al. 2013a; Sugimura et al. 2013b): (1) hydrogen-bonding attraction between residual hydroxyls of CE and VP-carbonyl groups of the vinyl (co)polymer; (2) steric hindrance of bulky side-groups to the interaction specified in (1); (3) indirect attraction via intramolecular repulsion between the comonomer units in the copolymer; and (4) weak interaction due to structural affinity (e.g., dipole-dipole antiparallel alignment) between the ester side-group of CE (such as CH_3-CH_2-CO-O-C-) and the VAc (-(CH_2-CH(-O-CO-CH_3))-) or MMA (-(CH_2-(CH_3)C(-CO-O-CH_3))-) unit. To explain the factor 3 more lucidly, when two monomer species having mutually repellent characters are randomly combined by covalent bonding, the copolymers tend to form a miscible phase with the CE component in the binary blends, rather than self-associate with the strong intramolecular repulsion. Unfortunately, however, the factors 3 and 4 could not be directly detected by the spectroscopic measurements.

In the present comparative study of the CE/vinyl polymer blends, we aim to clarify the contributions of the copolymer effect and structural affinity to the miscibility attainment, by another method besides thermal and spectroscopic techniques. In a previous work (Ohno and Nishio 2007b), we preliminarily estimated the attractive or repulsive action between chain segments of the polymer ingredients participating in the three systems, CA/P(VP-*co*-VAc), CA/P(VP-*co*-MMA), and CB/P(VP-*co*-VAc), in terms of Krigbaum-Wall polymer-polymer interaction parameters (Δb and μ) determinable by dilute solution viscometry. Particularly μ data gave a satisfactory account of the difference in the miscibility behaviour between the three blend systems (see later discussion). In this context, the present paper covers complementary assessments of μ parameters for various ingredient polymer pairs involved with the CP/P(VP-*co*-VAc) and CP/P(VP-*co*-MMA) systems. Through comprehensive comparison of the results with the μ data formerly obtained for the CA and CB systems, some profound insights are provided into the positive effect of propionyl

substitution leading to expansion of the miscible paring region in the maps of the CP systems. Additional attention is turned to miscibility behaviour of CB/P(VP-*co*-MMA) and cellulose acetate propionate (CAP)/P(VP-*co*-MMA) blends.

Experimental

Materials

CA was kindly provided from Daicel Corporation, and CAP was purchased from Eastman Chemical Co. CP and CB samples were synthesized with acid chloride/base catalyst from cotton cellulose via a homogeneous reaction in our laboratory, as has been described in the preceding papers (Nishio et al. 1997; Ohno and Nishio 2006; Kusumi et al. 2008). Table 1 summarizes the characterization data including DS, molecular weight, and glass transition temperature (T_g) determined by DSC (see below) for all the CE samples used in this study. Codes "CE_x" and "CA_yP_z" denote CE of ester DS = x and CAP of acetyl DS = y and propionyl DS = z, respectively.

<< **Table 1** >>

The vinyl polymers employed as a mixing partner for the CEs were PVP, PVAc, poly(methyl methacrylate) (PMMA), P(VP-*co*-VAc), and P(VP-*co*-MMA). Data of characterization for all the vinyl polymers are also listed in Table 1. As shown in the table, any of the copolymer samples exhibited a single T_g, and the T_g-copolymer composition relationships were in good obedience to a well-known Fox equation (Fox and Flory 1954), with a possible extent of scattering due to the difference in molecular weight; thus they were all regarded as essentially random copolymer. Hereafter, a P(VP-*co*-VAc) copolymer of VP:VAc = m:n (in molar ratio) is encoded as P(VP_m-*co*-VAc_n), and the same encoding rule is also applied for P(VP-*co*-MMA) samples.

145

146 Preparation of blend samples

147

148 Powder materials of CEs and vinyl polymers were individually dissolved in
149 *N*,*N*-dimethylformamide (DMF) at room temperature (~25 °C), at a polymer concentration of
150 1.00 g dL^{-1}. Blend solutions for viscometric measurements were prepared by mixing equal
151 amounts of two solutions of the component polymers. For DSC measurements, two
152 solutions of the required pairing polymers were mixed at the desired weight proportions.
153 The mixed polymer solutions (transparent) were then poured into a Teflon® tray and film
154 samples were made by evaporation of DMF at 50 °C under reduced pressure (< 10 mmHg).
155 The as-cast films were further dried at 50 °C *in vacuo* for 3 days, before supplying to the
156 thermal analysis.

157

158 Measurements

159

160 Viscosity measurements were performed for dilute polymer solutions in DMF with an
161 Ubbelohde capillary viscometer, which was placed in a thermo-regulated water bath (30 °C).
162 The temperature of the water bath was controlled within an accuracy range of ±0.1 °C. The
163 polymer concentration of the starting sample was adjusted to 1.00 g dL^{-1}, and dilutions of the
164 solutions were made to yield at least 4 lower concentrations by adding appropriate doses of
165 DMF. The measurements following the respective dilutions were done after elapsing of an
166 equilibrium time of 15 min. As for the polymer solutions containing $CP_{2.72}$ or $CB_{2.67}$,
167 however, the viscometric data were actually collected in a polymer concentration range below
168 ~0.30 g dL^{-1}, because the solutions of 1.00 g dL^{-1} were appreciably viscous due to
169 comparatively high molecular weights of the cellulosics (see Table 1). The elution time of
170 each solution from the set gauge of the viscometer was determined as the average of five

readings.

DSC thermal analysis was carried out with a Seiko DSC 6200/EXSTAR 6000 apparatus. The temperature readings were calibrated with an indium standard. The calorimetry measurements were conducted on ca. 5-mg film samples packed in an aluminum pan under a nitrogen atmosphere. Each sample was first heated from ambient temperature (~25 °C) to ~220 °C at a scanning rate of 20 °C min^{-1}, and then immediately quenched to −50 °C at a rate of 80 °C min^{-1}. Following this, the second heating scan was run from −50 °C to 230 °C at a rate of 20 °C min^{-1} to record stable thermograms. Thermograms presented in this paper were all obtained in the second heating scan, and the T_g was taken as a temperature at the midpoint of a baseline shift in heat flow characterizing the glass transition.

Results and discussion

Quantification of interaction parameters

Following the preceding work (Ohno and Nishio 2007b), we applied a viscometric method developed by Krigbaum and Wall (Krigbaum and Wall 1950) and other groups (Cragg and Bigelow 1955; Chee 1990), to assess the attractive or repulsive interactivity between the CE-vinyl polymer constituents focused so far in this series of blend studies. The result was greatly useful to understand the difference in miscibility behaviour between the blend systems, as embodied in a later discussion.

A viscometric interaction parameter, b, for a non-electrolyte dilute polymer solution (usually, in the concentration range lower than ~1.0 g dL^{-1}) is defined to fulfill a liner relationship given by the Huggins equation (Huggins 1942):

$$\eta_{sp}/c = [\eta] + bc \qquad (1)$$

where c is the solute concentration, and η_{sp} and $[\eta]$ are the so-called specific and intrinsic

viscosities, respectively. The b is assumed to reflect an interaction between chain molecules of the considered polymer and determined from a slope of the plot of η_{sp}/c vs. c. The parameter b is also related to the Huggins coefficient k by

$$b = k[\eta]^2 \qquad (2)$$

The k value generally ranges from 0.3 (in good solvents) to ~0.7 (in the Θ state) (Bohdanecký and Kovář 1982).

With regard to a blend solution of two different polymers in a common solvent, Equation (1) is applicable in a rewritten fashion:

$$\left(\eta_{sp}\right)_m / c_m = [\eta]_m + b_m c_m \qquad (3)$$

where the subscript m denotes "mixture", and b_m is a comprehensive viscometric interaction parameter that reflects an overall interaction involving three possible combinations of polymer chains of the same species (1-1 and 2-2) or not (1-2).

In this viscometric treatment, the polymer-polymer miscibility is estimated by comparison between an experimentally obtained value and an ideally calculated one of b_m. The former value, b_m^{ex}, is determined from the plot of $(\eta_{sp})_m/c_m$ vs. c_m for blend solutions of a given polymer pair. The latter ideal value, b_m^{id}, is calculated by the following equation (Krigbaum and Wall 1950):

$$b_m^{id} = w_1^2 b_{11} + w_2^2 b_{22} + 2 w_1 w_2 b_{12} \qquad (4)$$

where w_i is the weight fraction of component i in the polymer mixture, and b_{ij} is an interaction parameter between the molecular chain of polymer i and that of polymer j, and thereby a potential value of b_{12} may be given by

$$b_{12} = \sqrt{b_{11} \times b_{22}} \qquad (5)$$

Here, a Krigbaum-Wall interaction parameter, Δb, is defined as

$$\Delta b = b_m^{ex} - b_m^{id} \qquad (6)$$

If Δb is positive, the polymer 1 and polymer 2 are mutually attractive and therefore the pair is taken as miscible. Contrarily, if Δb is negative, the repulsive pair is considered to be

immiscible. When there is a large difference between $[\eta]$ values of both polymers ($[\eta]_1$ and $[\eta]_2$), the following alternative parameter μ as a standard in non-dimensional unit may be more useful to predict the miscibility between the two components (Chee 1990).

$$\mu = \frac{\Delta b}{\left([\eta]_2 - [\eta]_1\right)^2} \qquad (7)$$

The absolute value of μ, i.e., $|\mu|$, should represent the relative strength of attractive or repulsive interaction between the two component polymer molecules.

Table 2 summarizes data of $[\eta]$ and b parameters (b_m^{ex} and b_m^{id}) obtained by the viscometry for DMF solutions of CEs, vinyl polymers, and selected blending pairs of 50/50 composition, together with the polymer-polymer interaction parameters Δb and μ determined for the blends. The values of $[\eta]$ and b_m^{ex} were obtained directly from the reduced viscosity (η_{sp}/c) versus concentration plots, and those of b_m^{id}, Δb, and μ were calculated by the relevant equations ((4), (6), and (7)) given above. For comprehensive purposes, some data were quoted from the previous paper (Ohno and Nishio 2007b). As can be seen in the table, the $[\eta]$ values of the cellulosics and those of the vinyl (co)polymers are fairly far apart, and hence the standardized parameter μ is mainly used below for discussion on the interaction and miscibility between the blend constituents.

<< **Table 2** >>

Overview of μ records for CA and CB blends

First, we briefly review the preceding results of μ assessment for CA/P(VP-*co*-VAc), CB/P(VP-*co*-VAc), and CA/P(VP-*co*-MMA) blends (Ohno and Nishio 2007b). Figs. 4a, 4c, and 5a summarize simplified miscibility maps of the three blend systems, with addition of the illustrations in terms of μ data obtained for selected polymer combinations (DS of CEs, ~2.7; VP:VAc or MMA of copolymers, ~0.5:0.5) critical to the respective systems. The individual μ evaluations were in consistency with the respective miscibility mappings based on DSC

thermal analysis; viz., a positive μ value was obtained for miscible pairs of cellulosic/synthetic polymers, while immiscible blends all provided a negative μ value.

<< **Figure 4 (a) & (b) & (c)** >>

<< **Figure 5 (a) & (b)** >>

As exemplified for a highly butyrated CB/P(VP-*co*-VAc) series (Fig. 4c, right), the μ data concerned with the "three" constituting polymer ingredients made an order with respective to the degree of "immiscibility": PVP/PVAc (-4.23×10^{-2}) > $CB_{2.67}$/PVP (-1.43×10^{-2}) ≥ $CB_{2.67}$/PVAc (-1.07×10^{-2}). The mutually repellent character of the PVP/PVAc pair is considerably stronger than the corresponding ones of the other pairs $CB_{2.67}$/PVP and $CB_{2.67}$/PVAc. Then it can be taken for the $CB_{2.67}$/P($VP_{0.52}$-*co*-$VAc_{0.48}$) blend that the P(VP-*co*-VAc) component was intimately mixed with the CB component showing less repulsion to both the comonomer units, as a result of avoidance of the intense repulsion between VP and VAc segments inevitable in the copolymer-copolymer association; the blending pair of $CB_{2.67}$/P($VP_{0.52}$-*co*-$VAc_{0.48}$) is surely attractive to each other, giving a positive μ value, $+3.69\times10^{-3}$. This reasoning would satisfy us about the appearance of the miscibility window (Fig. 4c, left), as amplified in the following sections. On the other hand, such an explicit window never appeared in the map of the CA/P(VP-*co*-VAc) system (see Fig. 2a and 4a), although there should have arisen the intra-copolymer effect improving the miscibility in the blends of relatively high-acetylated CAs. The absence of the window may be interpreted as due to an inhibiting factor, i.e., the strong self-association ability of highly substituted CAs of DS > 2.7; the CAs are rather easily crystallizable as cellulose triacetate II form. Differing from this, no crystallizing habit was detected even for a CB synthesized at DS = 2.94 (Ohno and Nishio 2006). The lesser self-association nature of CB should be advantageous to that attractive interaction with the P(VP-*co*-VAc) component.

Meanwhile, another vinyl polymer combination of PVP and PMMA provided a μ value of -1.87×10^{-2}, from which the binary system is suggested to be immiscible. In fact, the

blend samples showed a common behaviour of essentially double T_gs in DSC measurements (Ohno and Nishio 2007b). However, the $|\mu|$ value for the PVP/PMMA pair is smaller than that ($|\mu| = 4.23\times10^{-2}$) for the PVP/PVAc pair. Thus it is deduced that the constituents VP and MMA in P(VP-*co*-MMA) show a somewhat weaker repulsive interaction than the VP and VAc units in P(VP-*co*-VAc). Presumably, this deterioration of the latent copolymer effect is responsible for the observation of a narrower miscible region in the CA/P(VP-*co*-MMA) map (Fig. 5a) relative to that in the CA/P(VP-*co*-VAc) map (Fig. 4a).

Inspection of miscibility maps for CP blends in μ terms

CP/P(VP-co-VAc) system

As shown in Fig. 4b (right), a negative μ value -1.02×10^{-2} was obtained for the combination of $CP_{2.72}$ and PVP homopolymer, while μ of the $CP_{2.72}$/P($VP_{0.52}$-*co*-$VAc_{0.48}$) pair was positive, $+1.50\times10^{-2}$. From these assessments, PVP and P($VP_{0.52}$-*co*-$VAc_{0.48}$) are taken as immiscible and miscible, respectively, with the highly esterified CP. The judgment is actually in accordance with the result of miscibility estimation by thermal analysis for the blends (see Fig. 4b, left). For another essential pair, $CP_{2.72}$/PVAc, we obtained a negative μ of -7.19×10^{-5}, but the absolute value is much smaller than that for the $CP_{2.72}$/PVP pair by more than two orders of magnitude. The former pair was previously marked to be partially miscible by observation of two T_gs approaching each other to an appreciable extent, and the low magnitude of μ reflects such a "better compatibility" of highly substituted CP with PVAc homopolymer.

Despite no presence of strong intermolecular attraction between $CP_{2.72}$ and the two homopolymers (PVP and PVAc), the CP component was able to be miscible with the copolymer comprising VP and VAc units. This phenomenon is explicable as being due to the more intense repulsive action between the VP and VAc segments in the P(VP-*co*-VAc)

copolymer component, as in the case of the CB/P(VP-*co*-VAc) system. We find for sure in Fig. 4b (right) that the PVP/PVAc pair shows the largest negative μ value (-4.23×10^{-2}) in the three polymer pairs participating in the $CP_{2.72}$/P(VP-*co*-VAc) system. In general, when two monomer species repelling each other are randomly combined by covalent bonding, the resulting copolymer tends to intimately mix with the other polymer of less self-associating nature, so as to reduce the strong repulsion between the comonomer units (ten Brinke et al. 1983; Paul and Barlow 1984). This is the reason why the high-esterified CP and CB can be miscible with P(VP-*co*-VAc) in a restricted range of the copolymer composition, even though there is a scarcity of specific attractive force (i.e. proton donor-acceptor interaction) between the two mixing components.

As is obvious in Fig. 4, the miscible region in the CP/P(VP-*co*-VAc) map is larger than the corresponding ones in the other maps of CA/P(VP-*co*-VAc) and CB/P(VP-*co*-VAc). In perspective comparison, the region involved in the CP system expands particularly to the side of VAc-richer compositions. This improvement virtually comes from the better compatibility of CP with PVAc supported above by the μ data of -7.19×10^{-5} for $CP_{2.72}$/PVAc. This value in $|\mu|$ is overwhelmingly small, compared with $\mu = -2.12\times10^{-2}$ for $CA_{2.70}$/PVAc (Fig. 4a, right) and $\mu = -1.07\times10^{-2}$ for $CB_{2.67}$/PVAc (Fig. 4c, right).

For three pairs of P($VP_{0.52}$-*co*-$VAc_{0.48}$) with the CEs of DS ≈ 2.7, we can rank them according to μ data, as follows: $CA_{2.70}$/P($VP_{0.52}$-*co*-$VAc_{0.48}$) ($+7.12\times10^{-2}$) > $CP_{2.72}$/P($VP_{0.52}$-*co*-$VAc_{0.48}$) ($+1.50\times10^{-2}$) > $CB_{2.67}$/P($VP_{0.52}$-*co*-$VAc_{0.48}$) ($+3.69\times10^{-3}$), all showing miscibility. The $CA_{2.70}$/P($VP_{0.52}$-*co*-$VAc_{0.48}$) pair exhibited the highest μ value, which is attributable to the direct interaction based on the actually detected hydrogen bonding between CA-hydroxyl and VP-carbonyl groups (Miyashita et al. 2002; Ohno et al. 2005); however, the increase of μ relative to that for $CA_{2.70}$/PVP ($+4.53\times10^{-2}$) suggests a secondary contribution of the intra-copolymer effect to the miscibility attainment. The hydrogen bonding effect seriously declines in the other two systems adopting propionyl and butyryl

substitutions for the CE component. Consequently, the miscibility of $CB_{2.67}$ with P($VP_{0.52}$-*co*-$VAc_{0.48}$) is realized only through the intra-copolymer repulsion as an indirect driving force. As to the $CP_{2.72}$/P($VP_{0.52}$-*co*-$VAc_{0.48}$) pair, besides the copolymer effect, a weak interaction due to structural affinity between the propionyl ester group and VAc unit also acts as a factor contributory to the miscibility attainment.

CP/P(VP-co-MMA) system

Fig. 5b (left) displays a simplified diagram of the miscibility mapping conducted for CP/P(VP-*co*-MMA) blends (Fig. 3b). In the right side of Fig. 5b, μ data are collected for four combinations of $CP_{2.72}$ with P($VP_{0.50}$-*co*-$MMA_{0.50}$), P($VP_{0.22}$-*co*-$MMA_{0.78}$), PVP, and PMMA, the values being $+9.33\times10^{-4}$, $+4.27\times10^{-3}$, -1.02×10^{-2}, and -3.23×10^{-4}, respectively. Judging from the positive or negative sign of μ, the P(VP-*co*-MMA) copolymers are taken as potentially miscible with $CP_{2.72}$, whereas both the homopolymers are not. These judgments entirely agree with the actual markings for the $CP_{2.72}$/P(VP-*co*-MMA) series in the miscibility map. In addition, PVP/PMMA blends are immiscible and this polymer pair provides a larger negative μ (-1.87×10^{-2}) than the $CP_{2.72}$/PVP and $CP_{2.72}$/PMMA pairs. The relationship in repulsion (immiscibility) between the three ingredient polymer pairs participating in the $CP_{2.72}$/P(VP-*co*-MMA) series is basically similar to that found for the $CP_{2.72}$/P(VP-*co*-VAc) series (see Fig. 4b, right). Accordingly, it is reasonable to assume that the intramolecular repulsive effect of the VP-MMA copolymer gave rise to the miscibility window in the map for the CP/P(VP-*co*-MMA) system. However, the window region observed for this system is obviously narrower than that for the CP/P(VP-*co*-VAc) system (see Fig. 4b, left). This narrowing of the window may be ascribed to the weaker repulsion in the VP-MMA copolymer relative to that in the VP-VAc copolymer ($\mu = -4.23\times10^{-2}$), as has been applied to the comparative discussion of the two maps for the corresponding blends of CA. The location of the window in the side of MMA-rich compositions owes to the better affinity

between CP and MMA segments, as supported by the lower order (10^{-4}) of μ obtained for the $CP_{2.72}$/PMMA pair.

Complementary mapping for CB/P(VP-*co*-MMA) system by application of μ assessment

In the miscibility characterization of CE/vinyl copolymer blends, we have not yet accomplished the total mapping for the CB/P(VP-*co*-MMA) system by thermal analysis. A main reason is that T_gs (ca. 110–120 °C) of CBs of DS ≈ 2.5–2.9 are fairly close to those (ca. 100–115 °C) of P(VP-*co*-MMA)s of VP < 50 mol%. However, we previously acquired the following data for the system concerned: (i) CB and PVP homopolymer formed miscible blends of hydrogen-bonding type unless the butyryl DS exceeded ~2.5 (see Fig. 2c) (Ohno and Nishio 2006); (ii) a polymer pair of CB (DS = 2.94) with P($VP_{0.50}$-*co*-$MMA_{0.50}$) was judged to be immiscible (double T_gs) (Ohno and Nishio 2007b).

To depict the miscibility map of the CB/P(VP-*co*-MMA) system more closely, we newly examined the blend miscibility of relatively low-substituted CBs (DS < 2.5) with P(VP-*co*-MMA)s by DSC and also quantified μ for additional pairs of CB (DS ≥ 2.6) with MMA-rich P(VP-*co*-MMA)s by viscometry. A major concern is whether the miscibility window emerges or not in the CB/P(VP-*co*-MMA) map.

Fig. 6a illustrates DSC thermograms measured for blend samples of $CB_{2.01}$/PMMA homopolymer; the binary cast films were mostly cloudy to the naked eye. As can be seen from the data, two independent glass transitions originating from the two components were detected for the 40/60–80/20 compositions (in wt% ratio), signalizing immiscibility of the $CB_{2.01}$/PMMA pair. The same behaviour of double T_gs was also observed for $CB_{2.41}$/PMMA blends. In contrast, Fig. 6b and c offer a typical miscible evidence in DSC (i.e. composition-dependent single T_g) for $CB_{2.01}$/P($VP_{0.22}$-*co*-$MMA_{0.78}$) and $CB_{2.01}$/P($VP_{0.50}$-*co*-$MMA_{0.50}$) blends, respectively. Similar miscible behaviour was

confirmed for other polymer combinations using $CB_{2.41}$ and/or P(VP-*co*-MMA)s of VP ≥ 9 mol% (MMA ≤ 91 mol%). Additionally, as-cast films of the CB blends with the P(VP-*co*-MMA)s were all highly transparent in the visual inspection. Thus it turns out that the lower limit in VP fraction of P(VP-*co*-MMA) that can be miscible with CB (DS < ~2.5) is ~10 mol%, which is almost the same limit as that found when CP was the CE component (see Fig. 5b). In a reasoning similar to that applied to interpret the CP/P(VP-*co*-MMA) map, the miscibility of CB with P(VP-*co*-MMA)s so rich in MMA residues (e.g. MMA = 87 and 91 mol%) would be invited by a good compatibility between the butyl ester side-group and the MMA unit. This may be supported by μ assessment of an extremely small negative value (-8.35×10^{-5}) for a polymer pair $CB_{2.67}$/PMMA (see Table 2).

<< **Figure 6 (a) & (b) & (c)** >>

In the present viscometric μ measurements, we found a definitely positive data such as $\mu = +2.12\times10^{-3}$ for $CB_{2.67}$/P($VP_{0.22}$-*co*-$MMA_{0.78}$). This indicates that even CB of DS > 2.5 is potentially miscible with the vinyl copolymer rich in MMA. Fig. 7 (left) summarizes a miscibility map constructed for the total system of CB/P(VP-*co*-MMA) by the combined use of the DSC and μ-assessment results. In the map, solid lines separate the miscible and immiscible regions connected with DS of CB and VP fraction of P(VP-*co*-MMA), to provide a miscibility window in the upper right portion. As illustrated in the right side in Fig. 7, μ parameters for three combinations of the ingredient polymers pertinent to the $CB_{2.67}$/P(VP-*co*-MMA) series are all negative, but the PVP/PMMA pair gives the largest absolute value (1.87×10^{-2}). This situation again supports the contribution of the intramolecular repulsion inherent in the P(VP-*co*-MMA) copolymer to the appearance of the miscibility window. However, the region is diminished to some extent, compared to the window in the CB/P(VP-*co*-VAc) map (Fig. 4c), because the repulsion between VP and MMA units is weaker than that between VP and VAc units, as already mentioned above.

<< **Figure 7** >>

Here we should further note that $CB_{2.67}$ of DS ≈ 2.7 is estimated to be immiscible with P($VP_{0.50}$-*co*-$MMA_{0.50}$) of VP:MMA = 50:50 from the μ data of -3.39×10^{-3}. In contrast, a comparable pair using CP, i.e., $CP_{2.72}$/P($VP_{0.50}$-*co*-$MMA_{0.50}$), was miscible, which was decisive from both T_g and μ determinations (see Figs. 3b and 5b). It follows, therefore, that the miscible pairing region (mainly associated with the window) in the CB/P(VP-*co*-MMA) map is a little narrower than that of the CP/P(VP-*co*-MMA) map. This comparison is made clearer in Fig. 7 (left), as guided by solid lines and broken ones inserted therein.

As indicated above, intimate mixing of two polymer components through the copolymer repulsion effect is unrealized on blending $CB_{2.67}$ with P($VP_{0.50}$-*co*-$MMA_{0.50}$). In interpretation of this, the following data should be recalled: $\mu = -1.87\times10^{-2}$ for PVP/PMMA and -1.43×10^{-2} for $CB_{2.67}$/PVP (see Fig. 7, right), the two values being close to each other. In the employment of the copolymer of VP = 50 mol%, probably, the relatively strong repulsion would still work between the CB component and the VP residue and inhibit the mutual approach of the two polymer components. Consequently, the intramolecular copolymer effect to attain miscible CB/P(VP-*co*-MMA) blends is active only at restricted copolymer compositions considerably rich in MMA. On the other hand, the repulsion between $CP_{2.72}$ and PVP ($\mu = -1.02\times10^{-2}$) is evidently weaker than that between PVP and PMMA (see Fig. 5b, right), and the copolymer effect would be significant even at the composition of VP = 50 mol%, resulting in the miscible blending of the $CP_{2.72}$/P($VP_{0.50}$-*co*-$MMA_{0.50}$) pair. In addition, a low frequency of intermolecular hydrogen-bondings might contribute to this miscibility attainment as a secondary effect. This inference took into consideration the DS boundary of ~2.7 partitioning the mixing states of CP/P(VP-*co*-MMA) blends (VP ≥ 60 mol%) (Fig. 5b, left).

Inspection of estimation results of miscibility for CAP/P(VP-*co*-MMA) blends in μ terms

Finally, we refer to miscibility behaviour of CAP blends with P(VP-*co*-MMA). To make a comparison with the result for the $CP_{2.72}$/P(VP-*co*-MMA) series, a partially acetylated cellulose propionate sample, $CA_{0.16}P_{2.52}$ (acetyl DS = 0.16; propionyl DS = 2.52), was selected as the mixed ester component.

Fig. 8 (left) collects the miscibility data (Sugimura et al. 2013b) based on thermal analysis for the target $CA_{0.16}P_{2.52}$/P(VP-*co*-MMA) blends, together with the corresponding data in the uses of $CP_{2.72}$ and $CA_{2.70}$. In the right side, an additional illustration is given in terms of μ assessment. The combination of $CA_{0.16}P_{2.52}$ and P($VP_{0.50}$-*co*-$MMA_{0.50}$) imparted a positive μ value of $+5.79\times10^{-3}$, while negative μ data of -1.01×10^{-2} and -2.08×10^{-4} were assigned to $CA_{0.16}P_{2.52}$/PVP and $CA_{0.16}P_{2.52}$/PMMA pairs, respectively. Therefore, the P($VP_{0.50}$-*co*-$MMA_{0.50}$) copolymer is potentially miscible with the mixed ester $CA_{0.16}P_{2.52}$, whereas both the homopolymers are not. These judgments are consistent with the results of miscibility estimation by DSC for the respective blends, also supporting that the $CA_{0.16}P_{2.52}$/P(VP-*co*-MMA) series offers a miscibility window, as did the blend series using $CP_{2.72}$. Furthermore, the immiscible polymer pair of PVP/PMMA provides a larger negative μ (-1.87×10^{-2}) than the other immiscible pairs of $CA_{0.16}P_{2.52}$/PVP and $CA_{0.16}P_{2.52}$/PMMA. From this triangular relationship, the intramolecular repulsive effect of the VP-MMA copolymer may be regarded as being responsible for the emergence of the miscibility window in the map for the CAP/P(VP-*co*-MMA) blends.

<< **Figure 8** >>

However, it is astonishing that the VP:MMA range involved in the window became more expanded in the $CA_{0.16}P_{2.52}$/P(VP-*co*-MMA) series, when compared with the situation in the $CP_{2.72}$/P(VP-*co*-MMA) series. In order to explain this expansion, we directed attention to another intramolecular repulsive interaction that might have arisen in the mixed ester component *per se*. Thereupon, a cellulose ester pair $CA_{2.70}$/$CP_{2.72}$ was explored by thermal analysis and viscometry for evaluations of the miscibility and interaction parameter; the

residual hydroxyl contents of the monoester derivatives ($CA_{2.70}$ and $CP_{2.72}$) are equalized to that of $CA_{0.16}P_{2.52}$. DSC measurements confirmed that $CA_{2.70}/CP_{2.72}$ blends exhibited dual T_g signals corresponding to those of the two constituents at any blending proportion. The Krigbaum-Wall interaction parameter of this polymer pair was estimated to be negative, as $\mu = -8.12\times10^{-3}$ (see Fig. 8, right), in conformity with the immiscible behaviour of the blends. The absolute value of this μ is appreciably large, although it is below $|\mu| = 1.87\times10^{-2}$ for the PVP/PMMA pair. The present result suggests that a relatively strong repulsive interactivity can work between the two cellulosic ester components.

In view of the above context, it is deduced that the cellulose mixed ester would also behave as a kind of copolymer dangling two different ester groups along the carbohydrate backbone; thus, the CAP/P(VP-*co*-MMA) blends are taken as a copolymer/copolymer system where the miscibility should be affected by the duplicated, intramolecular copolymer effect. The expansion of the window in the mapping of the $CA_{0.16}P_{2.52}$/P(VP-*co*-MMA) blends can be ascribed to such an additional repulsion effect originating in the CAP side.

Conclusions

The blend miscibility of CP with the VP-containing vinyl copolymers P(VP-*co*-VAc) and P(VP-*co*-MMA) is improved in respect of the miscible pairing number, compared with the cases using CA and CB. This behaviour was satisfactorily explained by comparing the attractive or repulsive interactivities between related polymer ingredients in terms of the Krigbaum-Wall interaction parameter μ that was determined by solution viscometry. Especially, great contributions of both the intra-copolymer effect and the structural affinity effect to the miscibility attainment were made clear by the μ assessments. The former effect is explicitly responsible for the miscibility window appearing in the maps constructed for the CP/vinyl copolymer systems, and this is also applicable to the maps for the CB systems.

The comparatively narrower window observed when the counter component to CP or CB was P(VP-*co*-MMA) is interpretable as due to the lesser strength in repulsion of the VP-MMA copolymer relative to that of the VP-VAc copolymer. The structural affinity effect is concretely connected with a good compatibility of the propionyl group of CP with the VAc or MMA unit of the partner copolymer in the CP-based two systems, and, in the employment of CB, this effect is active between the butyryl and MMA moieties in the CB/P(VP-*co*-MMA) system only.

Such a useful μ measurement was also applied to the inspection of miscibility mapping for CAP blends with P(VP-*co*-MMA). The observed expansion of the miscibility window relative to that for the comparable CP blends was explicable in terms of the μ data, which indicated additional repulsion in the side of the cellulose mixed ester component; therefore, the CAP/P(VP-*co*-MMA) blends should be taken as a copolymer/copolymer system where the duplicated copolymer effect works.

From a practical standpoint, the present results will be so useful for related researchers to expand the opportunities of material design based on the CE family including cellulose mixed esters. Delicate characterization and even prediction of the miscibility may be possible for many other series of CE/synthetic copolymer blends by examining the viscometric interaction parameters of the targeted constituent polymer pairs, in addition to the orthodox thermal and spectroscopic estimations.

Acknowledgements

This work was financed by a Grant-in-Aid for Research Activity Start-up (No. 25892017 to KS) as well as by a Grant-in-Aid for Scientific Research (A) (No. 26252025 to YN) from the Japan Society for the Promotion of Science.

Compliance with Ethical Standards

The authors declare no conflict of interest.

Reference

Bohdanecký M, Kovář J (1982) Viscosity of Polymer Solutions. Elsevier, Amsterdam

Chee KK (1990) Determination of polymer-polymer miscibility by viscometry. Eur Polym J 26:423–426.

Cragg LH, Bigelow CC (1955) The Viscosity Slope Constant k′—Ternary Systems: Polymer–Polymer–Solvent. J Polym Sci 16:177–191.

Edgar KJ, Buchanan CM, Debenham JS, Rundquist PA, Seiler BD, Shelton MC, Tindall D (2001) Advances in cellulose ester performance and application. Prog Polym Sci 26:1605–1688.

Fox TG, Flory PJ (1954) The Glass Temperature and Related Properties of Polystyrene. Influence of Molecular Weight. J Polym Sci 14:315–319.

Hayakawa D, Ueda K (2015) Computational study to evaluate the birefringence of uniaxially oriented film of cellulose triacetate. Carbohydr Res 402:146–151.

Higeshiro T, Teramoto Y, Nishio Y (2009) Poly(vinyl pyrrolidone-*co*-vinyl acetate)-*graft*-poly(ε-caprolactone) as a Compatibilizer for Cellulose Acetate/Poly(ε-caprolactone) Blends. J Appl Polym Sci 113:2945–2954.

Huggins M (1942) The Viscosity of Dilute Solutions of Long-Chain Molecules. IV. Dependence on Concentration. J Am Chem Soc 64:2716–2718.

Krigbaum WR, Wall FT (1950) Viscosities of binary polymeric mixtures. J Polym Sci 5:505–514.

Kusumi R, Inoue Y, Shirakawa M, Miyashita Y, Nishio Y (2008) Cellulose alkyl ester/poly(ε-caprolactone) blends: characterization of miscibility and crystallization behaviour. Cellulose 15:1–16.

Liu Y, Huglin MB, Davis TP (1994) Preparation and characterization of some liner

copolymers as precursors to thermoplastic hydrogels. Eur Polym J 30:457–463.

Miyashita Y, Suzuki T, Nishio Y (2002) Miscibility of cellulose acetate with vinyl polymers. Cellulose 9:215–223.

Nishio Y (2006) Material Functionalization of Cellulose and Related Polysaccharides via Diverse Microcompositions. Adv Polym Sci 205:97–151.

Nishio Y, Matsuda K, Miyashita Y, Kimura N, Suzuki H (1997) Blends of poly(ε-caprolactone) with cellulose alkyl esters: effect of the alkyl side-chain length and degree of substitution on miscibility. Cellulose 4:131–145.

Ohno T, Nishio Y (2006) Cellulose alkyl ester/vinyl polymer blends: effects of butyryl substitution and intramolecular copolymer composition on the miscibility. Cellulose 13:245–259.

Ohno T, Nishio Y (2007a) Molecular Orientation and Optical Anisotropy in Drawn Films of Miscible Blends Composed of Cellulose Acetate and Poly(*N*-vinylpyrrolidone-*co*-methyl methacrylate). Macromolecules 40:3468–3476.

Ohno T, Nishio Y (2007b) Estimation of Miscibility and Interaction for Cellulose Acetate and Butyrate Blends with *N*-Vinylpyrrolidone Copolymers. Macromol Chem Phys 208:622–634.

Ohno T, Yoshizawa S, Miyashita Y, Nishio Y (2005) Interaction and Scale of Mixing in Cellulose Acetate/Poly(*N*-vinyl Pyrrolidone-*co*-vinyl Acetate) Blends. Cellulose 12:281–291.

Paul DR, Barlow JW (1984) A binary interaction model for miscibility of copolymers in blends. Polymer 25:487–494.

Rustemeyer P (ed) (2004) Cellulose Acetates: Properties and Applications. Wiley-VCH, Weinheim

Sugimura K, Katano S, Teramoto Y, Nishio Y (2013a) Cellulose propionate/poly(*N*-vinyl pyrrolidone-*co*-vinyl acetate) blends: dependence of the miscibility on propionyl DS and

copolymer composition. Cellulose 20:239–252.

Sugimura K, Teramoto Y, Nishio Y (2013b) Blend miscibility of cellulose propionate with poly(*N*-vinyl pyrrolidone-*co*-methyl methacrylate). Carbohydr Polym 98:532–541.

Sugimura K, Teramoto Y, Nishio Y. Cellulose Acetate. In: Kobayashi S, Müllen K (eds) Encyclopedia of Polymeric Nanomaterials. Springer, Berlin/Heidelberg, in press. doi: 10.1007/978-3-642-36199-9_328-1

ten Brinke G, Karasz FE, MacKnight WJ (1983) Phase Behavior in Copolymer Blends: Poly(2,6-dimethyl-1,4-phenylene oxide) and Halogen-Substituted Styrene Copolymers. Macromolecules 16:1827–1832.

Yamaguchi M (2010) Optical Properties of Cellulose Esters and Their Blends. In: Lejeune A, Deprez T (eds) Cellulose: Structure and Properties, Derivatives, and Industrial Uses. Nova Science Publishers, New York, pp 325–340

Yamaguchi M, Manaf MEA, Songsurang K, Nobukawa S (2012) Material design of retardation films with extraordinary wavelength dispersion of orientation birefringence: a review. Cellulose 19:601–613.

Yamanaka H, Teramoto Y, Nishio Y (2013) Orientation and Birefringence Compensation of Trunk and Graft Chains in Drawn Films of Cellulose Acetate-*graft*-PMMA Synthesized by ATRP. Macromolecules 46:3074–3083.

Yoshitake S, Suzuki T, Miyashita Y, Aoki D, Teramoto Y, Nishio Y (2013) Nanoincorporation of layered double hydroxides into a miscible blend system of cellulose acetate with poly(acryloyl morpholine). Carbohydr Polym 93:331–338.

584
585 **Figure Captions**

586

587 **Fig. 1** Structural formulae of (a) CEs (i.e., CA, CP, and CB), (b) P(VP-*co*-VAc), and (c)
588 P(VP-*co*-MMA).

589

590 **Fig. 2** Miscibility maps for three blend systems (a) CA/P(VP-*co*-VAc) (Miyashita et al.
591 2002), (b) CP/P(VP-*co*-VAc) (Sugimura et al. 2013a), and (c) CB/P(VP-*co*-VAc) (Ohno and
592 Nishio 2006), depicted as a function of DS of CE and VP fraction of the copolymer in a
593 rearranged fashion with additional data. Symbols indicate that a given pair of CE/vinyl
594 polymer is miscible (○, single T_g), immiscible (×, dual T_gs), or partially miscible (△, dual
595 T_gs approaching each other to an appreciable degree).

596

597 **Fig. 3** Miscibility maps for two blend systems (a) CA/P(VP-*co*-MMA) (Ohno and Nishio
598 2007b) and (b) CP/P(VP-*co*-MMA) (Sugimura et al. 2013b), depicted as a function of DS of
599 CE and VP fraction of the copolymer in a rearranged fashion with additional data. The
600 meanings of two symbols ○ and × are the same as defined in Fig. 2.

601

602 **Fig. 4** Miscibility maps (left) with additional illustrations using μ data (right) for (a)
603 CA/P(VP-*co*-VAc), (b) CP/P(VP-*co*-VAc), and (c) CB/P(VP-*co*-VAc) systems. The meanings
604 of three symbols ○, ×, and △ are the same as used in Fig. 2. The miscibility maps are
605 represented in a simplified style retaining the essence of the data shown in Fig. 2.

606

607 **Fig. 5** Miscibility maps (left) with additional illustrations using μ data (right) for (a)
608 CA/P(VP-*co*-MMA) and (b) CP/P(VP-*co*-MMA) systems. The meanings of two symbols ○
609 and × are the same as used in Fig. 2. The miscibility maps are represented in a simplified
610 style retaining the essence of the data shown in Fig. 3.

Fig. 6 DSC thermograms obtained for blends of $CB_{2.01}$ with (a) PMMA, (b) P($VP_{0.22}$-*co*-$MMA_{0.78}$), and (c) P($VP_{0.50}$-*co*-$MMA_{0.50}$). Arrows indicate a T_g position taken as the midpoint of a baseline shift in heat flow.

Fig. 7 Miscibility map (left) and additional illustration (right) using μ data for CB/P(VP-*co*-MMA) blends. The meanings of two symbols ○ and × are the same as used in Fig. 2. Solid lines in the map represent a boundary partitioning the miscible and immiscible regions for the CB/P(VP-*co*-MMA) system, and, for comparison, the corresponding boundary for the CP/P(VP-*co*-MMA) system (Fig. 5b) is drawn by broken lines.

Fig. 8 Mapping of miscibility data (Sugimura et al. 2013b) (left) and additional illustration in μ terms (right) for $CA_{0.16}P_{2.52}$/P(VP-*co*-MMA) blends. For comparison, miscibility data for the corresponding blends using $CA_{2.07}$ and $CP_{2.72}$ (see Fig. 3) are also mapped in the left figure. The meanings of two symbols ○ and × are the same as used in Fig. 2.

In addition to the eight figures, there are two tables. See annexed sheets.

631
632 **Table 1** Characterization of CEs and synthetic vinyl polymers used in the present study

Sample code [a]	M_w [d]	M_n [d]	M_w/M_n [d]	T_g/°C	Source
$CP_{2.72}$	1,070,000	367,000	2.92	134	Synthesized
$CA_{0.16}P_{2.52}$	258,000	73,400	3.51	143	Eastman Chemical Co.
$CA_{2.70}$	237,000	73,000	3.25	186	Daicel Co.
$CB_{2.67}$	998,000	285,000	3.50	114	Synthesized
$CB_{2.41}$	952,000	218,000	4.37	132	Synthesized
$CB_{2.01}$	651,000	294,000	2.21	139	Synthesized

Sample code	M_w [e]	M_n [e]	M_w/M_n [e]	T_g/°C	Source
PVP	24,500 [f]	–	–	162	Nacalai Tesque, Inc.
PVAc	90,000 [f]	–	–	41	Polyscience, Inc.
P($VP_{0.52}$-*co*-$VAc_{0.48}$) [b]	28,000	5,120	5.47	89	Polyscience, Inc.
PMMA	88,400	35,000	2.53	100	Aldrich Chemical Co.
P($VP_{0.22}$-*co*-$MMA_{0.78}$) [c]	189,000	70,800	2.66	111	Synthesized [g]
P($VP_{0.50}$-*co*-$MMA_{0.50}$) [c]	184,000	61,300	3.00	119	Synthesized [g]

[a] The DS values were determined by ^{1}H NMR.

[b] The VP content was determined by ^{1}H NMR.

[c] The VP contents were determined by FT-IR in a way described by Liu et al. (1994).

[d] Determined by gel permeation chromatography (mobile phase, tetrahydrofuran at 40 °C) with polystyrene standards.

[e] Determined by gel permeation chromatography (mobile phase, 10 mM L^{-1} lithium bromide/DMF at 40 °C) with polystyrene standards.

[f] Nominal value.

[g] Synthesized in the authors' laboratory by radical polymerization of two distilled monomers, VP (Nacalai Tesque, Inc.) and MMA (Nacalai Tesque, Inc.), in the same way as that described in a previous paper (Ohno and Nishio 2007b).

633 **Table 2** Data of intrinsic viscosity and interaction parameters estimated by viscometry for

634 CEs, synthetic vinyl polymers, and their respective 50/50 blends

Samples	$[\eta]$/dL·g^{-1}	b_m^{ex}/dL^2·g^{-2}	b_m^{id}/dL^2·g^{-2}	Δb/dL^2·g^{-2}	μ
$CP_{2.72}$	6.27	1.84×10^{1}	–	–	–
$CA_{0.16}P_{2.52}$	1.85	1.84	–	–	–
$CA_{2.70}$ [a]	2.28	1.86	–	–	–
$CB_{2.67}$ [a]	5.61	1.13×10^{1}	–	–	–
PVP [a]	1.46×10^{-1}	1.18×10^{-2}	–	–	–
PVAc [a]	6.10×10^{-1}	1.32×10^{-1}	–	–	–
P($VP_{0.52}$-*co*-$VAc_{0.48}$) [a]	1.67×10^{-1}	1.21×10^{-2}	–	–	–
PMMA [a]	2.92×10^{-1}	3.01×10^{-2}	–	–	–
P($VP_{0.22}$-*co*-$MMA_{0.78}$)	3.64×10^{-1}	3.45×10^{-2}	–	–	–
P($VP_{0.50}$-*co*-$MMA_{0.50}$) [a]	5.54×10^{-1}	9.47×10^{-2}	–	–	–
$CP_{2.72}$/PVP	3.77	4.46	4.85	-3.84×10^{-1}	-1.02×10^{-2}
$CP_{2.72}$/PVAc	3.42	5.42	5.42	-2.30×10^{-3}	-7.19×10^{-5}
$CP_{2.72}$/P($VP_{0.52}$-*co*-$VAc_{0.48}$)	3.20	5.41	4.85	$+5.59\times10^{-1}$	$+1.50\times10^{-2}$
$CP_{2.72}$/PMMA	3.67	4.98	4.99	-1.15×10^{-2}	-3.23×10^{-4}
$CP_{2.72}$/P($VP_{0.22}$-*co*-$MMA_{0.78}$)	3.09	5.17	5.02	$+1.49\times10^{-1}$	$+4.27\times10^{-3}$
$CP_{2.72}$/P($VP_{0.50}$-*co*-$MMA_{0.50}$)	3.12	5.32	5.29	$+3.05\times10^{-2}$	$+9.33\times10^{-4}$
$CA_{0.16}P_{2.52}$/PVP	9.80×10^{-1}	5.06×10^{-1}	5.35×10^{-1}	-2.91×10^{-2}	-1.01×10^{-2}
$CA_{0.16}P_{2.52}$/PMMA	1.07	5.83×10^{-1}	5.84×10^{-1}	-5.03×10^{-4}	-2.08×10^{-4}
$CA_{0.16}P_{2.52}$/P($VP_{0.50}$-*co*-$MMA_{0.50}$)	1.13	7.01×10^{-1}	6.91×10^{-1}	$+9.71\times10^{-3}$	$+5.79\times10^{-3}$
$CA_{2.70}$/PVP [a]	1.38	7.50×10^{-1}	5.43×10^{-1}	$+2.07\times10^{-1}$	$+4.53\times10^{-2}$
$CA_{2.70}$/PVAc [a]	1.47	6.87×10^{-1}	7.47×10^{-1}	-5.95×10^{-2}	-2.12×10^{-2}
$CA_{2.70}$/P($VP_{0.52}$-*co*-$VAc_{0.48}$) [a]	1.61	8.63×10^{-1}	5.44×10^{-1}	$+3.20\times10^{-1}$	$+7.12\times10^{-2}$
$CA_{2.70}$/PMMA [a]	1.28	5.85×10^{-1}	5.92×10^{-1}	-6.64×10^{-3}	-1.67×10^{-3}
$CA_{2.70}$/P($VP_{0.50}$-*co*-$MMA_{0.50}$) [a]	1.40	6.78×10^{-1}	6.99×10^{-1}	-2.12×10^{-2}	-7.06×10^{-3}
$CB_{2.67}$/PVP [a]	2.97	2.59	3.01	-4.27×10^{-1}	-1.43×10^{-2}
$CB_{2.67}$/PVAc [a]	3.14	3.20	3.47	-2.69×10^{-1}	-1.07×10^{-2}
$CB_{2.67}$/P($VP_{0.52}$-*co*-$VAc_{0.48}$) [a]	2.82	3.13	3.02	$+1.10\times10^{-1}$	$+3.69\times10^{-3}$
$CB_{2.67}$/PMMA [a]	3.04	3.13	3.13	-2.37×10^{-3}	-8.35×10^{-5}
$CB_{2.67}$/P($VP_{0.22}$-*co*-$MMA_{0.78}$)	2.42	3.21	3.15	$+5.84\times10^{-2}$	$+2.12\times10^{-3}$
$CB_{2.67}$/P($VP_{0.50}$-*co*-$MMA_{0.50}$) [a]	3.16	3.28	3.37	-8.67×10^{-2}	-3.39×10^{-3}
PVP/PVAc [a]	3.90×10^{-1}	4.66×10^{-2}	5.57×10^{-2}	-9.13×10^{-3}	-4.23×10^{-2}
PVP/PMMA	2.40×10^{-1}	1.95×10^{-2}	1.99×10^{-2}	-4.02×10^{-4}	-1.87×10^{-2}
$CA_{2.70}$/$CP_{2.72}$	4.34	7.88	8.01	-1.29×10^{-1}	-8.12×10^{-3}

[a] Data were quoted from a previous paper (Ohno and Nishio 2007b).

635

636

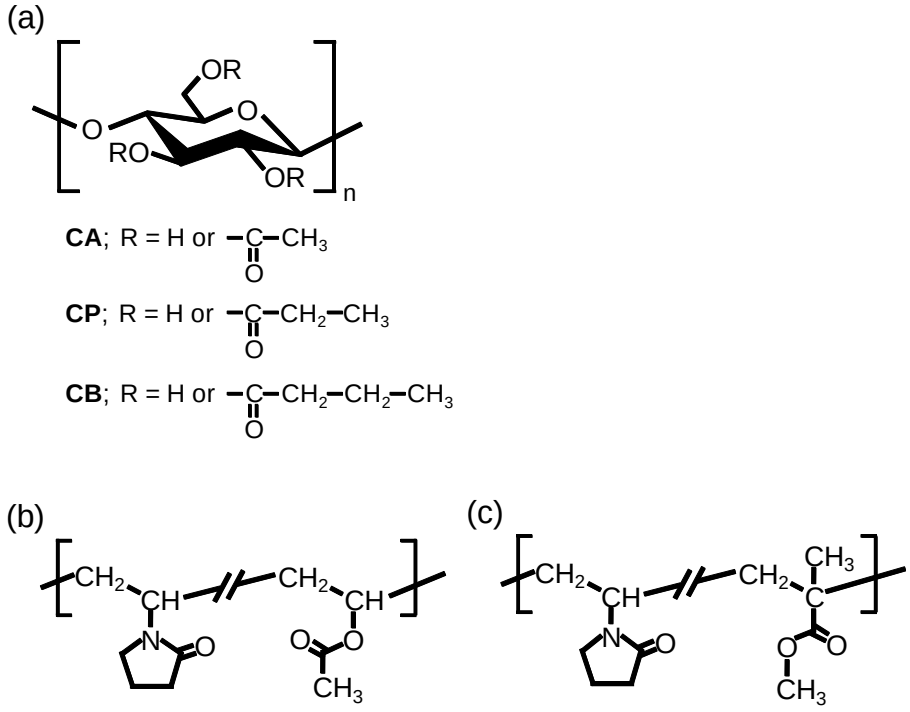

637

638

639

640 **Fig. 1** Structural formulae of (a) CEs (i.e., CA, CP, and CB), (b) P(VP-*co*-VAc), and (c)

641 P(VP-*co*-MMA).

642

643

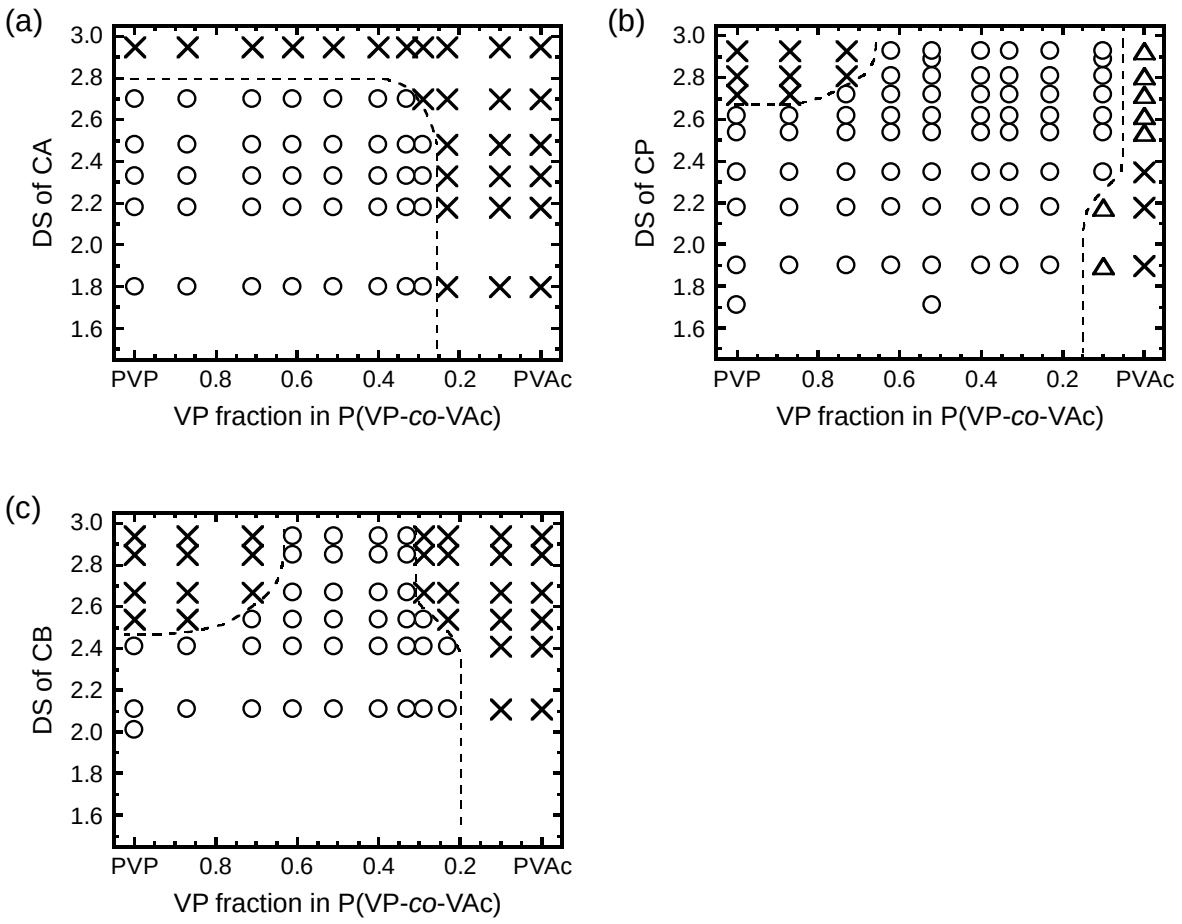

Fig. 2 Miscibility maps for three blend systems (a) CA/P(VP-*co*-VAc) (Miyashita et al. 2002), (b) CP/P(VP-*co*-VAc) (Sugimura et al. 2013a), and (c) CB/P(VP-*co*-VAc) (Ohno and Nishio 2006), depicted as a function of DS of CE and VP fraction of the copolymer in a rearranged fashion with additional data. Symbols indicate that a given pair of CE/vinyl polymer is miscible (○, single T_g), immiscible (×, dual T_gs), or partially miscible (△, dual T_gs approaching each other to an appreciable degree).

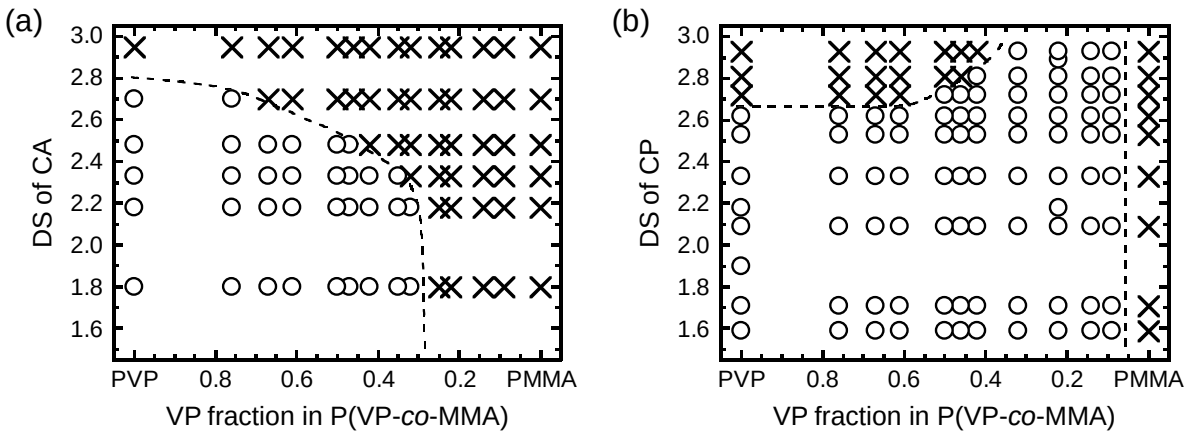

Fig. 3 Miscibility maps for two blend systems (a) CA/P(VP-*co*-MMA) (Ohno and Nishio 2007b) and (b) CP/P(VP-*co*-MMA) (Sugimura et al. 2013b), depicted as a function of DS of CE and VP fraction of the copolymer in a rearranged fashion with additional data. The meanings of two symbols ○ and × are the same as defined in Fig. 2.

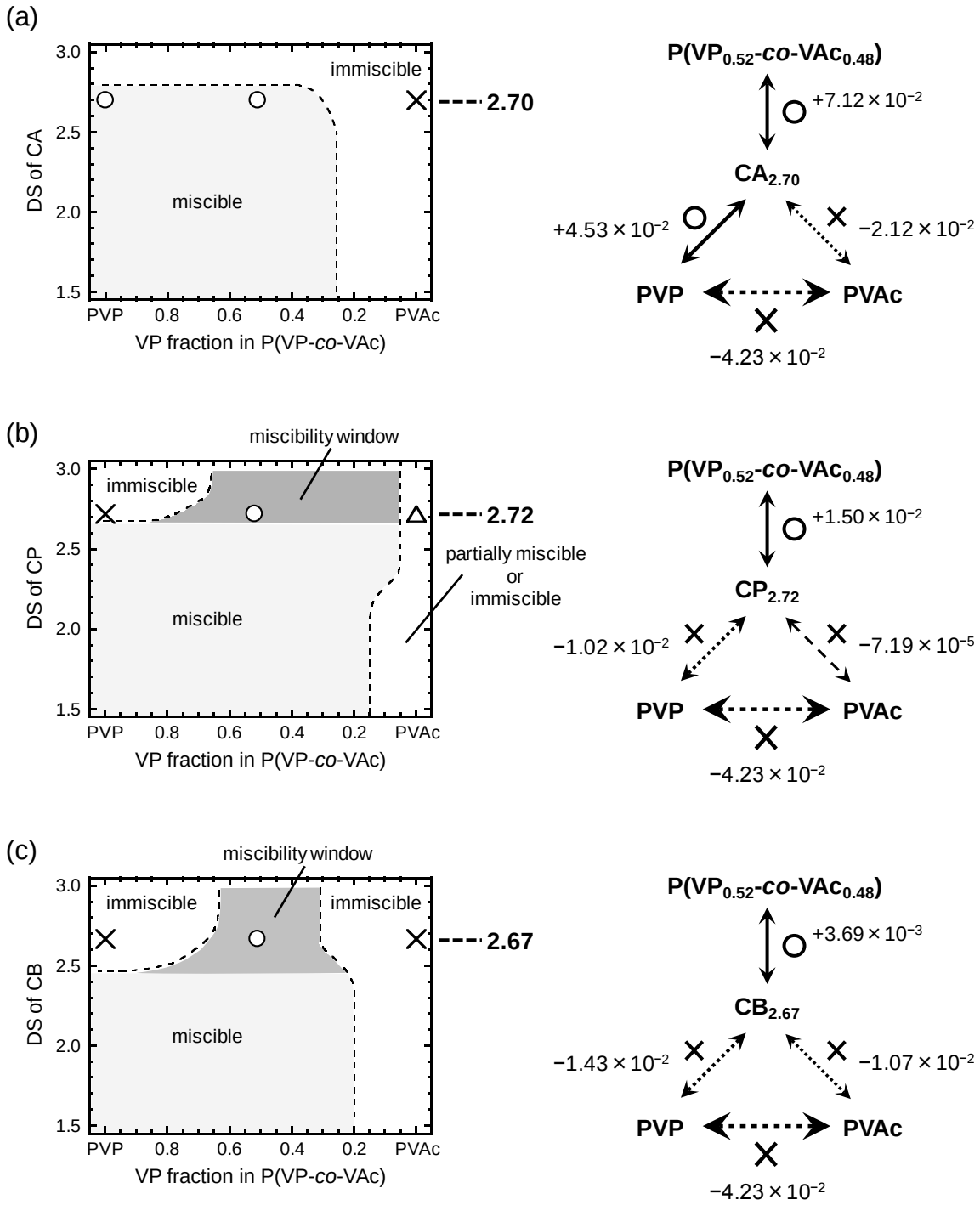

Fig. 4 Miscibility maps (left) with additional illustrations using μ data (right) for (a) CA/P(VP-*co*-VAc), (b) CP/P(VP-*co*-VAc), and (c) CB/P(VP-*co*-VAc) systems. The meanings of three symbols ○, ×, and △ are the same as used in Fig. 2. The miscibility maps are represented in a simplified style retaining the essence of the data shown in Fig. 2.

673

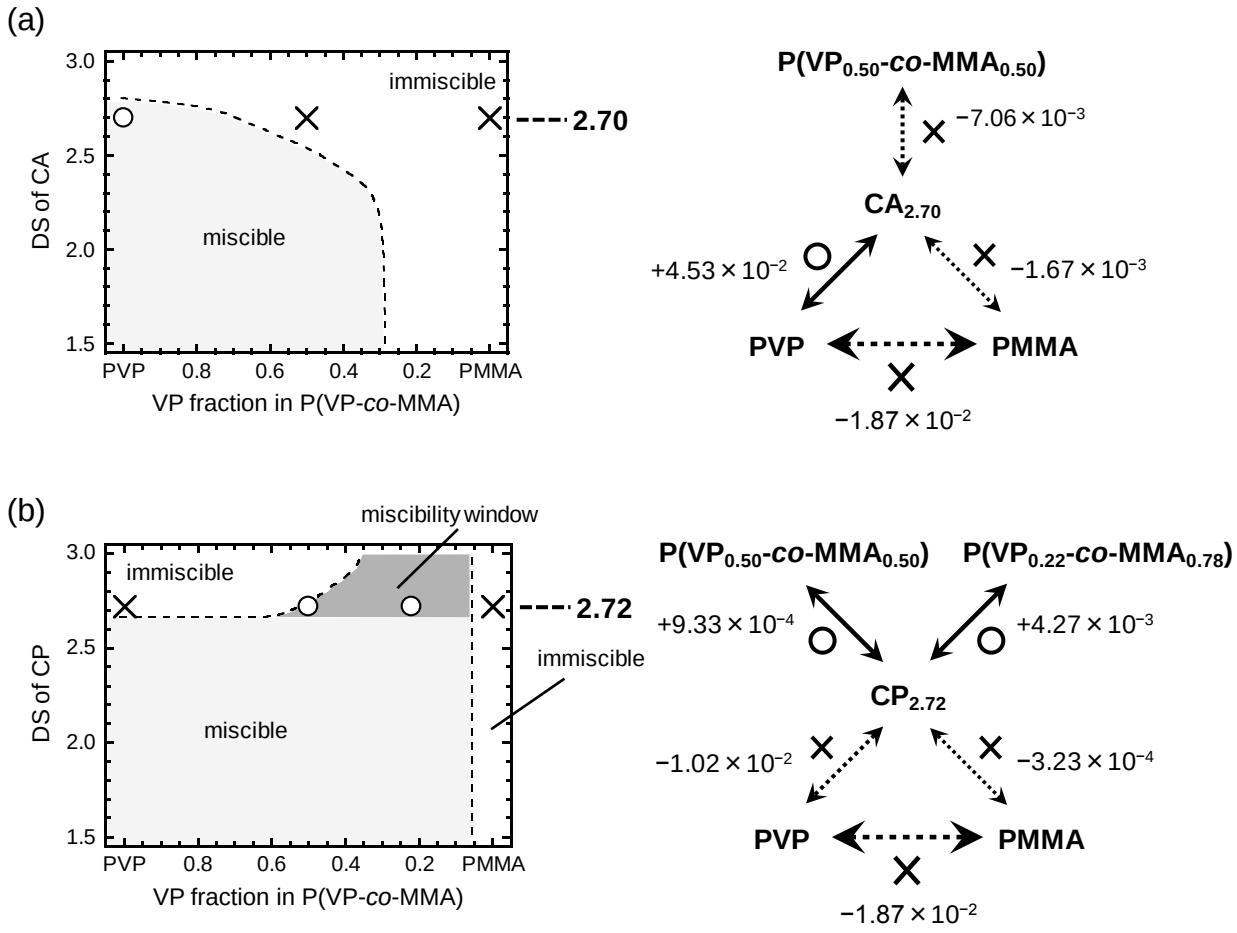

674

675

676

677 **Fig. 5** Miscibility maps (left) with additional illustrations using μ data (right) for (a)
678 CA/P(VP-*co*-MMA) and (b) CP/P(VP-*co*-MMA) systems. The meanings of two symbols ○
679 and × are the same as used in Fig. 2. The miscibility maps are represented in a simplified
680 style retaining the essence of the data shown in Fig. 3.

681

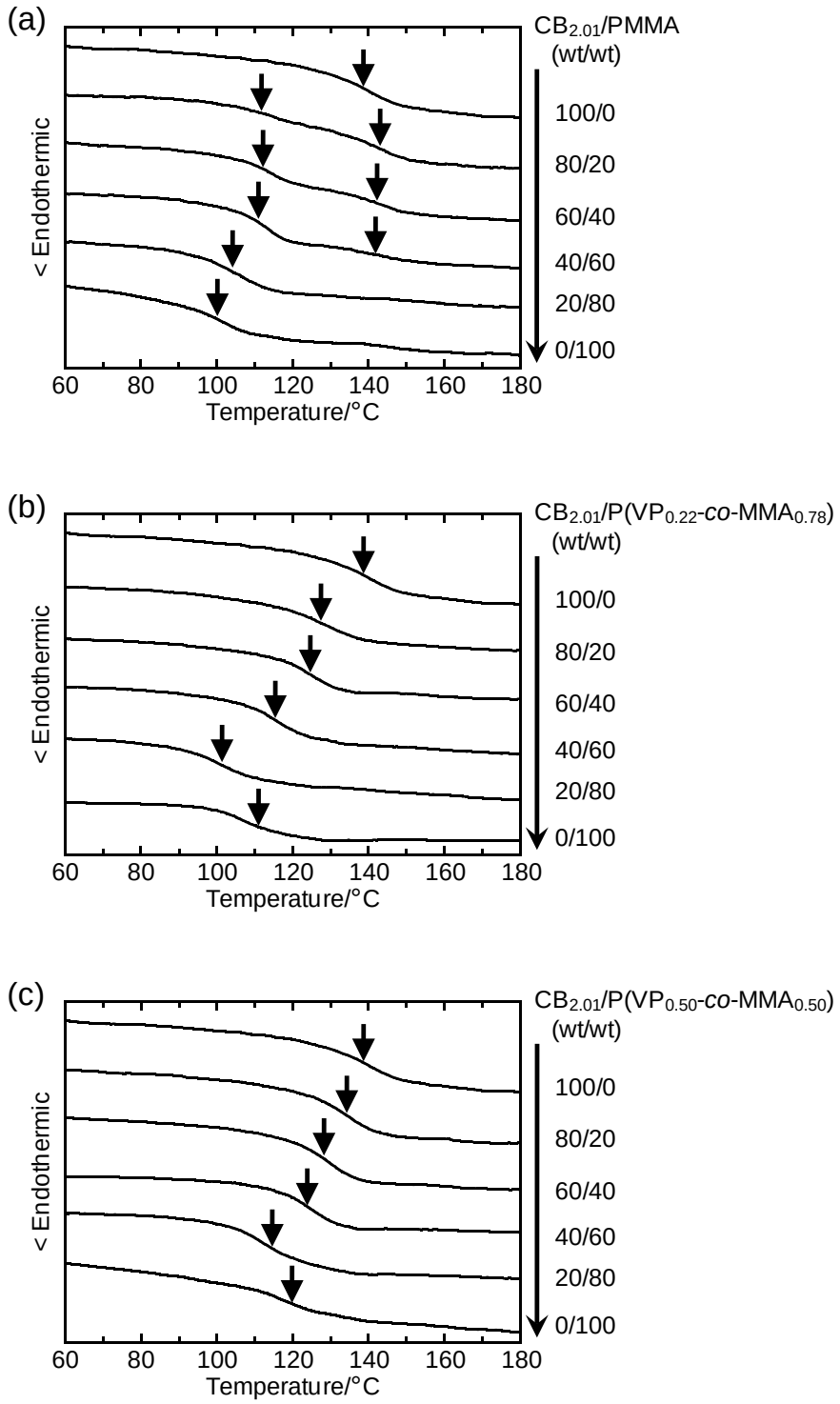

Fig. 6 DSC thermograms obtained for blends of $CB_{2.01}$ with (a) PMMA, (b) $P(VP_{0.22}$-*co*-$MMA_{0.78})$, and (c) $P(VP_{0.50}$-*co*-$MMA_{0.50})$. Arrows indicate a T_g position taken as the midpoint of a baseline shift in heat flow.

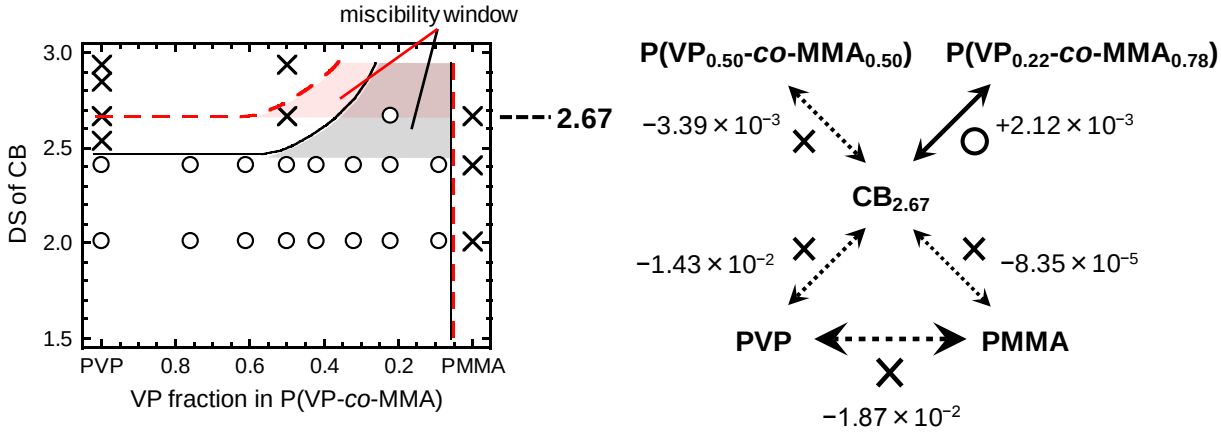

Fig. 7 Miscibility map (left) and additional illustration (right) using μ data for CB/P(VP-*co*-MMA) blends. The meanings of two symbols ○ and × are the same as used in Fig. 2. Solid lines in the map represent a boundary partitioning the miscible and immiscible regions for the CB/P(VP-*co*-MMA) system, and, for comparison, the corresponding boundary for the CP/P(VP-*co*-MMA) system (Fig. 5b) is drawn by broken lines.

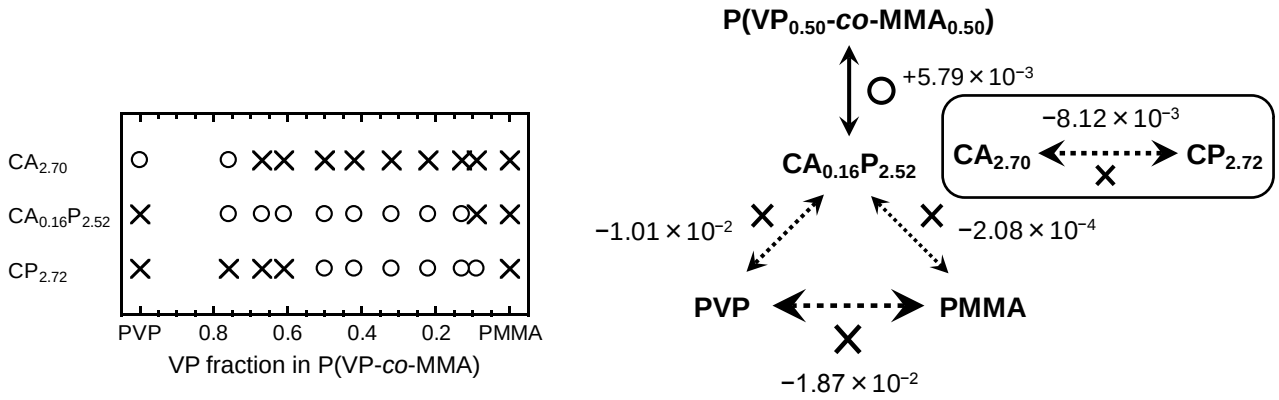

Fig. 8 Mapping of miscibility data (Sugimura et al. 2013b) (left) and additional illustration in μ terms (right) for $CA_{0.16}P_{2.52}$/P(VP-*co*-MMA) blends. For comparison, miscibility data for the corresponding blends using $CA_{2.07}$ and $CP_{2.72}$ (see Fig. 3) are also mapped in the left figure. The meanings of two symbols ○ and × are the same as used in Fig. 2.